

Urban road pavements monitoring and assessment using bike and e-scooter as probe vehicles

Salvatore Cafiso¹, Alessandro Di Graziano², Valeria Marchetta,
Giuseppina Pappalardo^{*3}

Department of Civil Engineering and Architecture, University of Catania, Via S. Sofia, 64, I-95123 Catania, Italy



ARTICLE INFO

Keywords:
Road pavement
Bike
E-scooter
Vibration
Smartphone

ABSTRACT

Comfort and safe-mobility are two aspects that should be provided to non-motorized users that are an increasing component of the urban micro-mobility (e.g. bikes and e-scooters). For these road users, road pavement unevenness, cracks, potholes and other surface defects can make riding uncomfortable and potentially hazardous. Traditionally, road managers use standardized surveys and Key Performance Indicators (KPIs) of pavement to make decision for maintenance programs and pavement management of road urban network poses challenges in the survey of pavement surface for International Roughness Index (IRI) and distress assessment both for operational and cost constraints. Moreover, there are theoretically limitations of IRI model for low speed urban roads and low-damped vehicles like bikes and e-scooters. In such framework aims of the paper is to investigate the use of smartphone sensors to collect data for the assessment of pavement conditions and definition of KPIs for bike and e-scooter users' ride comfort and safety. A controlled experiment was performed with repeated runs of a bicycle and e-scooter equipped with a smartphone and an android application was used to collect acceleration and position data. Detailed pavement conditions have been identified with an advanced survey equipment. After data treatments for removing signal noise, adjustment for speed variability and outlier detection, root mean square (RMS) of vertical acceleration signal and weighted frequency content of the vibrations according to ISO 2631-1, have been confirmed suitable KPIs of pavement conditions and comfort rating that can be collected by bikes and e-scooter. Results confirmed the lack of correlation of vibrations in bikes and e-scooter with analogous parameters collected with car as probe vehicle and with IRI standard values, as well. Instead, pavement monitoring by bikes and e-scooter can provide effective detection of typologies and severities of distresses not detectable by similar approaches in damped vehicles. Good correlations have been identified between RMS and medium severity alligator, longitudinal and transversal cracks. High severity pavement distress and potholes have been identified by outliers in RMS.

* Corresponding author.

E-mail addresses: decafiso@dica.unict.it (S. Cafiso), adigraziano@unict.it (A. Di Graziano), valeria.marchetta96@gmail.com (V. Marchetta), giusy.pap@dica.unict.it (G. Pappalardo).

¹ ORCID: 0000-0002-7247-0365

² ORCID: 0000-0001-6484-2758

³ ORCID: 0000-0002-9793-1885

<https://doi.org/10.1016/j.cscm.2022.e00889>

1. Introduction

Cities are facing with traffic issues such as congestion, noise pollution and greenhouse gas emissions. In response to these pressing issues, policy-makers are increasingly looking for ways to develop a more sustainable and flexible transport system, and influence behaviors to encourage a shift away from the reliance on private cars. The use of bike and e-scooter is increasingly viewed as a key part of a multi-modal and integrated transport system for several reasons, because they are environmentally, socially and economically sustainable [1].

While the planning and implementation of well-designed and safe infrastructure measures may encourage bike and e-scooter use, other factors will be important in determining the success of these infrastructure, such as the location of facilities along usable commuting routes; the overall network connectivity and the public's perception of how safe and comfortable it is to ride. Comfort and safe-mobility are two aspects that should be provided to this non-motorized users [2]. In such framework, road pavement is one of the major assets of urban roadway systems to be considered. Cracks, potholes, bumps, and other surface defects can degrade riding comfort and vehicle stability [3–5]. Maintenance and rehabilitation of pavement asset to preserve and achieve an acceptable level of service is a difficult challenge for urban road management [6] and the development of "non-motorized" users is highlighting new needs. In this context, the continuous evolution of technology offers interesting prospective of having a large amount of quality data available, collected at a lower cost [7]. Data collected with smartphone of different users followed by crowdsensing and mining have a cost lower and not comparable with traditional pavement survey techniques providing also a wider coverage and real time monitoring. This has the potential to improve road asset management by better supporting decision making based on a more comprehensive understanding of asset performance. All this is even more evident in the urban context, which has always been characterized by lack of information due to the extension and characteristics of the road network and traffic conditions which imply high costs for surveys and tailored key performance indicators (KPIs). These benefits, however, are not automatic. It is currently complex for road agencies to understand which available technology is suitable for large-scale applications and how to move to new approaches where existing processes and systems are adapted to the status quo (e.g. KPIs, thresholds for treatments) [8].

Traditionally, road managers use standardized surveys and KPIs of pavement to make decision about maintenance needs. International Roughness Index (IRI) is the most developed and well-known KPI of the pavement surface roughness introduced by the World Bank in 1984 as a standardized measure of a reference passenger car (golden car) ride comfort at a reference speed of 80 km/h related to the longitudinal profile.

However, use of IRI for low speed roads (e.g. urban roads) and no-passenger cars (e.g. bike) is cause of concerns.

The gain response to road profile slope, given by the quarter car model used to compute the IRI, at different roughness wavelengths/frequencies is plotted in Fig. 1, that is familiar to pavement engineers. From Fig. 1 it is evident how the use of the quarter car model neglects the effects of short wavelengths, reducing the estimation of body vibrations in a frequency range that is relevant for comfort especially at low speeds (e.g. $f > 10$ Hz at 50 km/h and $f > 5$ Hz at 20 km/h), typical of urban roads and for bikes or e-scooters.

Moreover, the spring/damper mass model of the quarter car cannot be directly applied to vehicle with no or limited suspension systems like bike and e-scooter. Fig. 2 shows the variability in the amplitude of vibration in a spring/damper mass system (equivalent to the quarter car model) for different damping ratios (ζ) that can vary from undamped ($\zeta = 0$) to overdamped ($\zeta > 1$). It is evident in Fig. 2, that the amplitude of the response is affected by the frequency of excitation ω and it increases dramatically for low damped systems especially for frequency ratios $\omega/\omega_n < 1$ (ω_n system natural frequency) that are typical of ride vibrations for bike and e-scooter.

While the lack of cycling quality infrastructure was already acknowledged by some previous studies as the main factor affecting cycling comfort [11–13], few studies are available for e-scooter mobility and not directly linked to detailed road pavement conditions [14,15].

Also, in the perspective to incentive more sustainable mobility modes, the previous considerations, well known in the literature, highlight the needs for KPIs more suitable for urban roads and for no-motorized users who are very sensible to comfort levels offered by the pavement surface of their paths. Moreover, severe pavement defects can be associated to hazard for vehicle stability and control.

In such framework, aim of the paper is to investigate the use of smartphone to collect data useful for the assessment of pavement

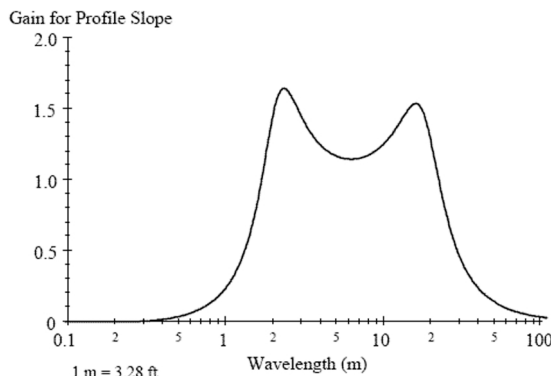


Fig. 1. Response of the IRI filter.

conditions and definition of KPIs for bike and e-scooter users' ride comfort. A controlled in field experiment was performed with repeated runs of a bicycle and e-scooter equipped with a smartphone and app to collect acceleration and position data, while detailed pavement conditions were collected with advanced survey equipment (Automatic Road Analyzed ARAN 9000). Procedures for data treatment, results for comfort assessment and correlations with pavement conditions are presented in the paper that is organized as follow:

- Literature review of previous studies focusing on the use of smartphone for pavement condition assessment
- Data collection and reporting to merge smartphone signal and pavement conditions
- Data processing for cleaning raw data from noise and outliers, speed correction and KPIs computation
- Analysis and results about existence of correlation with pavement surface distress typology and severity
- Conclusions with lessons learned and recommendations

2. Literature review

In literature there are many works on the use of smartphone sensors as a data source for pavement evaluation. Because the target of the paper is not an extensive literature presentation, in the following selected studies are reported as reference of the general approach and results in the field. Two of the most used devices sensor are the triaxial accelerometer and the Global Navigation Satellite System (GNSS) which together allow to collect data on the travel path and movements [16]. With these low cost sensors, by increasing both the monitoring and maintenance estimation, the needs of a pavement treatments can be identified promptly, reducing costs and increasing the serviceability of the road asset [17–19].

Several studies were carried on for detecting pavement singularities, like road bumps and potholes, based on the analysis of high-energy event in vertical acceleration impulse [20–23].

Other researchers have focused on the use of smartphone sensors for evaluating the roughness of the pavement surface and by using the vertical acceleration recorded by a mobile device in a car [23,24]. The International Roughness Index (IRI) was the more investigated parameter and the road surface condition classified by IRI-proxy factors.

In identifying the conditions of the pavement, the effect of speed in the study of vertical acceleration must be considered. In this regard, Alessandroni et al. [25] showed how the average value of vertical acceleration is closely related to vehicle speed. The authors developed the "SmartRoadSense" system which aims to monitor road surfaces via smartphones, using a model to calculate an index for the roughness of the pavement. In the same way, Zeng et al. [26] developed a normalized acceleration-based metric for different functional classes of highway by incorporating vehicle speed.

Although in the literature there are many works relating to the use of mobile sensors for monitoring road surfaces, there are few studies that deal with the evaluation of the pavement performance for non-motorized light transport.

Two Android based applications such as Roodroid [27] or Rovi [28] have been developed for the evaluation of road conditions, also allowing to select the type of vehicle, including bikes, so as to assign a different algorithm to each one for the evaluation of the surface conditions by the way of accelerations and image analysis.

Instrumented bikes capable of monitoring several key variables related to cycling, such as speed, steering and acceleration have been used to analyze how the irregularities on the pavement surface are perceived by the cyclists [29–32]. Li et al. [33] found strong correlations between pavement macro-texture (Mean Profile depth, MPD) and bicycle vibration and ride quality, but weak correlations with IRI.

Shtayat et al. [34] proposed a pavement monitoring system using a smartphone in the car with focus mainly on mining the crowd sensed data to carry out separated segment based IRI-proxy and localized transient events. Anyway, results have been validated against qualitative rating of pavement conditions. Similarly, Meocci et al. [35] propose both a local index to detect localized moderate/high

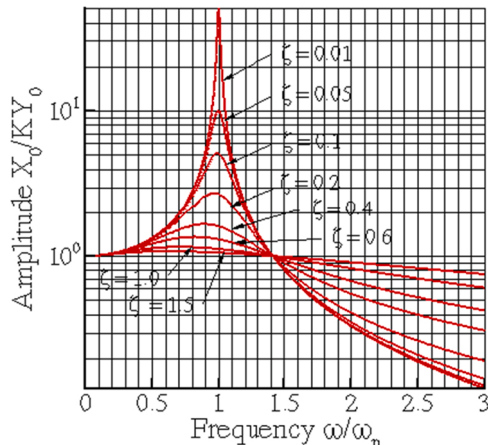


Fig. 2. Amplitude plot for a spring mass system with different damping ratio [9,10].

severity distresses (e.g. potholes) and a global distress index derived by the average value of vertical accelerations collected with different surveys, that showed a good correlation with the Pavement Condition Index visually estimated over a 100 m long section.

Collecting data from several users, even if in the same route, can generate different measurement, mainly because they can use different paths and the GNSS accuracy positioning is in the range of meters. Therefore, implementation of crowdsensing and mining, followed by spatial clustering, has been proposed as a suitable solution [36].

An extensive review of 130 papers [37] pointed out an increasing trend of applying artificial intelligence (AI) method, especially Machine Learning techniques, for detection of road anomalies, mainly applied to image analysis. Neural Network (NN)/Artificial Neural Network (ANN) and Support Vector Machine (SVM) are the most common methods applied to data collected by onboard sensors (e.g. speed, vertical displacement and acceleration). Most of studies used ML to detect potholes/humps and estimate roughness (e.g. IRI) [37–39]. Limited works are related to detailed distress detection and classification or by using micro-mobility rather than motorized vehicles. One of the conclusions was that AI techniques are promising but the disadvantage on high quality data dependence have limited their application.

As general consideration, the use of smartphone as system to collect data to be related to pavement conditions is widely studied and results consolidated for motorized vehicles (e.g. passenger car, bus), but there is still value in providing further studies to define KPI for bike and e-scooter along with a detailed assessment of pavement conditions including both longitudinal profile, widespread surface defects of different typologies and high severity localized pavement defects.

3. Methodological approach

As pavement conditions cause vibrations, an experiment was conducted using a smartphone to record the vertical accelerations and positions of a passenger car, a bicycle and an e-scooter and pavement surface conditions noted in detail. Collected vertical accelerations were pre-processed before analysis to remove noise, outliers and effects of different running speeds. GNSS NMEA (National Marine Electronics Association) data were used to identify vehicle speed and position and too much acceleration and pavement data. Correlations with pavement conditions and consistency of comfort ranking were tested for each vehicle in the experiment. We applied statistical tests of goodness of regression fitting, Generalized Linear Model for residual estimation and outlier's identification, ANOVA and t-test for paired comparison of repeated measures and Pearson or Spearman's rank correlation to analyze results and support

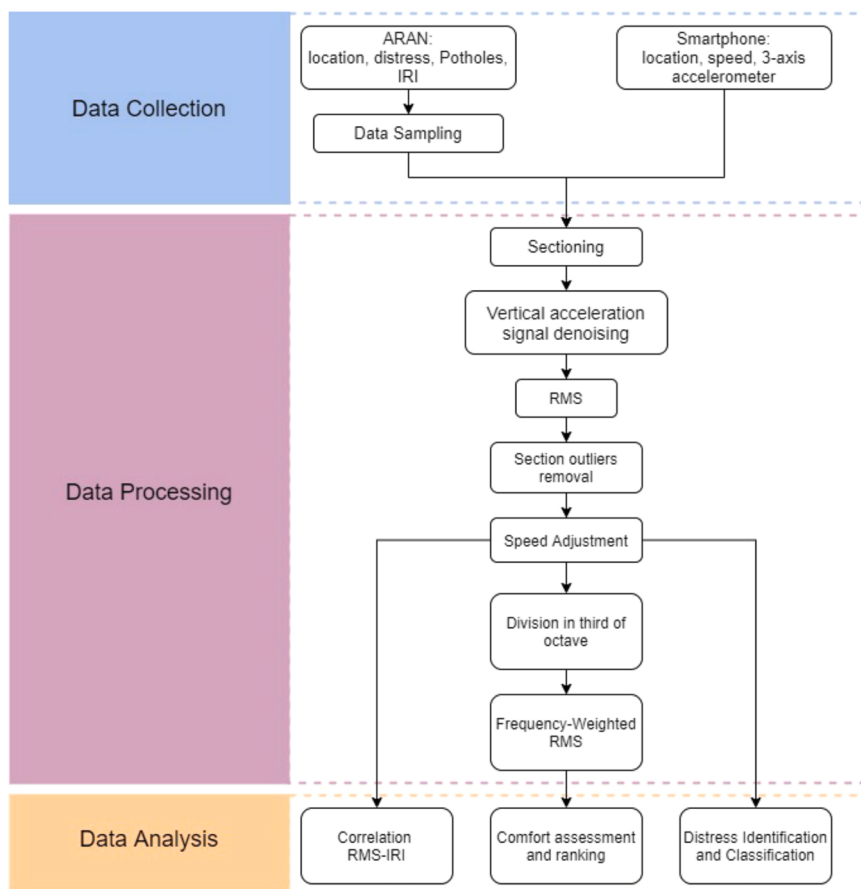


Fig. 3. Data processing and analysis flowchart.

conclusions. Fig. 3 shows the work flow from data collection to treatment and analysis.

3.1. Data collection

We carried out a controlled experiment at different speeds recording vertical accelerations and GNSS position to locate the data of the different runs with reference to fixed road sections of 10 m length.

Considering that the vibration perceived on board a vehicle varies according to the nature of the vehicle itself, the test was replicated with three different vehicles: car, bike and e-scooter. Bike and e-scooter are the focus of the study, while car was included for comparison reasons. Repeated measures were carried out at different speeds on a road stretch of 1100 m. The test was carried out on lanes of urban roads shared with motor vehicles. Anyway, the procedure may be particularly effective on bike lane, where the standard monitoring vehicles cannot operate. We carried out 10 tests at almost constant speeds equal to 12 km/h (2 runs), 17 km/h, 22 km/h and 25 km/h with the bike, 12 km/h, 14 km/h, 15 km/h and 20 km/h with the e-scooter and 50 km/h with the car.

To record simultaneously acceleration, position and speed data, the Android app "HyperIMU®" was installed on a Huawei P20lite smartphone, that was firmly attached to the vehicles with one accelerometer axis in vertical direction (Fig. 4).



Fig. 4. Equipment setting for inventory data collection.

The data on the condition of pavement, in terms of IRI and distress typology, extension and severity, were collected with the Automatic Road Analyzer (ARAN) of the University of Catania, that uses an advanced Laser Cracking Measurement System (LCMS) to detect, classify, and measure several distresses with millimeter precision [40]. The Automatic Road Analyzer (ARAN) is one of the most advanced equipment that allow to collect data from pavement and infrastructure features, using several synchronized sub-systems (SOP (Standard Operating Procedures) Laser, SmalTexture measurement system, LCMS measurement system, DGNSS (Differential Global Navigation Satellite System), DMI (Distance Measurement Instrument) and 3 cameras). The VISION® software provided by FUGRO® and Pavemetrics® has an advanced distress detection tool which combining the laser data with pavement images. The resulting 3D texture of the pavement surface contains detailed information for detecting, measuring and classifying different distresses based on a flexible setting of several parameters that need operator expertise and calibration trials. LCMS can be used for identification and rating a large amount of distresses, including potholes, longitudinal, transversal, alligator cracking, rutting, patching, etc (Fig. 5).

For the analysis, short sections of 10-meter length were adopted to have a detailed analysis of distress and vibration assessment. Along the test track, the road lane width was 3.0 m with a shoulder of 0.25 m. The test rider was instructed to travel on the right side of the lane within a strip of about 1.0 m wide. Therefore, for bike and e-scooter we considered only the distresses and IRI localized in such path identified by the blue lines in Fig. 5. Instead, for the car the average value of IRI (IRI_{avg}) in the right and left wheel paths (red dot lines in Fig. 5) and the total lane surface distress must be considered.

Pavement surface distress were classified in Longitudinal, Transversal and Alligator cracking with 3 severity classes (Table 1). The extension measure of the distress is based on the area (square meter) for Alligator Cracking (AC) and potholes, the length (meter) for longitudinal and transversal cracking. The severity classification has been done according to FHWA distress manual [41] that classify as Low a crack with mean width < 6 mm, as Moderate any crack with mean width > 6 mm and < 19 mm, as High any crack with mean width > 19 mm. Low was a pothole with deep < 25 mm, Moderate with deep < 50 mm and High with deep > 50 mm.

Table 1 shows a widespread presence of cracking with 61 out of 111 road sections with low and/or moderate alligator cracking, covering about 10% of the whole pavement surface in the test path of bike and e-scooter, nothing that width and pattern of low severity cracking are difficult to detect with visual human inspections, but they may be influential for bike and e-scooter vibrations.

Longitudinal and transversal cracking with width > 6 mm and length > 0.2 m (i.e. Moderate and High severity) have been detected in 63 sections. Potholes of low and moderate severity have been detected in 5 pavement sections. Finally, 27% of the test path (i.e. 30 out of 111 sections) was without any distress classified in the Moderate or High severity levels. It is worthy to mention that LCMS is very sensible detecting also short cracks (the minimum length was set at 0.20 m) of 2 mm width classified at low severity.

IRI ranges from good (i.e. $IRI < 2.0 \text{ m/km}$) to very poor (i.e. $IRI > 12.6 \text{ m/km}$) values. As the road profile encompasses a spectrum of sinusoidal wavelengths in different octave bands of frequency that have different effects on vehicle vibrations, the power spectral density (PSD) of profile displacement according to ISO 8608 [42] is also shown in the Fig. 6.

The two paths in the S-N and N-S directions are very similar in terms of pavement profile. The PSDs show a higher content in the octave band range $0.02 \div 0.125 \text{ cycle/m}$ (i.e. wavelengths > 8 m) associated with classes D-E of ISO and mainly effecting IRI values. The presence of PSD also in the higher frequency bands is evident and expected for a pavement surface characterized by widespread cracking, but less effecting IRI while relevant for body vibration and comfort especially at the lower speeds. The only difference between the two PSDs is below the $0.03\text{c}/\text{m}$ octave band which has little effect on both IRI and comfort [43]. The loose of PSD information for wave number higher than 4 and lower than $0.015\text{c}/\text{m}$ is due to the low and high pass filters usually applied to the longitudinal profile data for IRI computation [44]. The distress assessment and PSD analysis returned an overall evaluation of a pavement surface in moderate severity conditions, but with enough variability among typology and severity levels in the different test

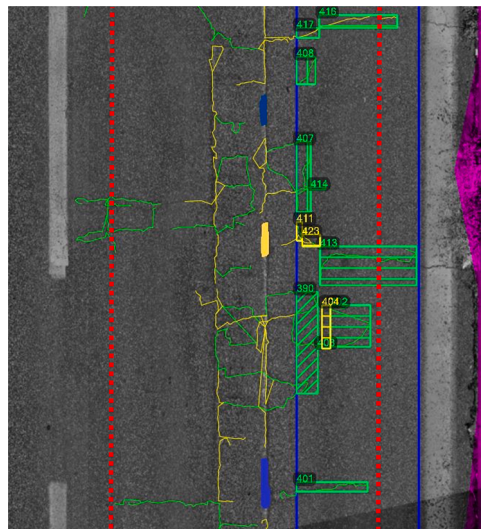
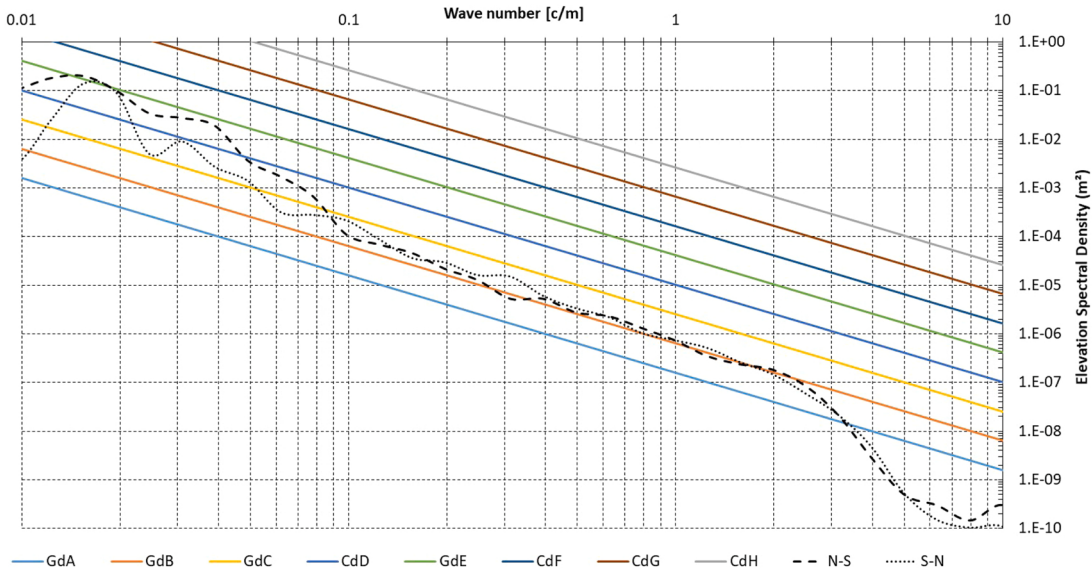


Fig. 5. Example of Distress detection and classification (Blue lines: bike and e-scooter test track. Dotted red lines: right and left IRI profiles). (For interpretation of the references to colour in this figure, the reader is referred to the web version of this article.)

Table 1

Descriptive Statistics of pavement Distresses in the bike wheel path.

Distress	Units	Severity	Min	Max	Avg	SD	Count
Transversal Cracking TC	m	Low	.25	6.60	1.87	1.49	83
		Moderate	.23	.89	.56	.32	32
		High	.30	.46	.38	.11	2
Longitudinal Cracking LC	m	Low	0.20	7.38	1.62	1.40	66
		Moderate	.22	5.33	1.11	1.14	54
		High	.27	1.13	.66	.38	6
Alligator Cracking AC	% m ²	Low	2%	52%	16%	11%	45
		Moderate	2%	47%	14%	10%	23
		High	—	—	—	—	0
Potholes	m ²	Low	.16	.16	.16	.16	1
		Moderate	.03	.12	.06	.06	5
		High	.29	.29	.29	.29	1
IRI_Right	m/km		1.00	15.83	4.17	2.79	111
IRI_Left (only for car)	m/km		1.48	15.84	5.05	2.72	111
MPD	mm		0.29	0.76	0.41	0.09	111

**Fig. 6.** Power Spectral Density of Elevation road profile.

samples to provide a useful test track for the experiment.

3.2. Data processing

We recorded acceleration signals in the time domain, so the first step was to translate the data into the space domain of the pavement sections to be able to match the signal of vertical acceleration with the distress and IRI data. This was possible by aligning the GNSS coordinates and chainage distance recorded from both the devices.

The signal recorded by the smartphone could be affected by noise linked to various factors, such as device performance and additional vibrations due to the anchoring system of the equipment to the vehicle. Noise is a broadband signal with a random trend over time that overlaps the useful signal and influences its intelligibility then the wavelet transform denoising process was applied in order to eliminate the background noise [45].

For the definition of vibrations transmitted to the body due to road conditions, ISO 2631-1 [46] is the reference standard. In accordance with this ISO standard, the Root Mean Square (RMS) of the vertical acceleration for each 10-meter section was chosen as reference KPI for the pavement condition:

$$RMS = \sqrt{\frac{1}{N} \sum_{i=1}^N x_i^2} \quad (1)$$

in which:

- N is the number of x_i values within the 10 m. road section;
- x_i is the i^{th} value of the vertical acceleration recorded, net of the average value of the vertical gravitational acceleration recorded in the test (9.8 m/s^2).

3.3. Outlier identification

Although the test path has been defined within a width of 1.0 m on the right side of the lane (Fig. 5), in the repeated tests, variability in the trajectory of the bike and e-scooter, within the one-meter path, is however possible. Moreover, preliminary data visualization showed the presence of peaks in the signal and anomaly values of RMS in single sections, but not always in each run.

To identify outliers and further to carry out an ANOVA to compare RMS values in the different surveys, we applied the Generalized Linear Model (GLM) for repeated measures to handle correlated non-independent data that do not satisfy the basic hypothesis on independence in the standard statistical tests. The GLM Repeated Measures procedure provides residuals and analysis of variance when the same measurement is made several times and, therefore, it is the most appropriate for analyzing our data collected in the different ride tests on the same road sections.

Outliers are single data points within our data that do not follow the usual pattern for RMS. The GLM paired comparison is effective to identify outliers through the observation of studentized residuals (SRs). Studentized is the residual of the i^{th} observation divided by an estimate of standard deviation with the i^{th} observation deleted. As general rule, if an observation has a SR larger than 3 (in absolute value) we can classify the observation as outlier, because the deviation of residual is larger than 3 standard deviations (i.e. 99.7% level of confidence or at least 89% for no normal distribution). It is worthily to mention that outliers, in our experiment, should be mainly associated to pavement singularity (e.g potholes, gutters, service covers, bumps, etc.) rather than system errors. Anyway, generally bicyclists and e-scooter riders try to avoid such localized severe pavement distress which produce abrupt increase in vertical accelerations. Moreover, our study target is mainly to evaluate the general pavement conditions and roughness as factor effecting ride comfort, even if localized severe pavement distress or other surface imperfections may be more relevant for safety, as well. Therefore, we decided to remove outliers from the general data analysis, when not repeatedly measured in the same road section, because they increase variability and reduce statistical power. Afterwards, we will handle outliers to investigate their underlying cause related to the pavement distress type and severity.

We have identified 33 outliers out of 535 samples in the 5 bike tests, the most severe (e.g. $\text{SR} > 3$) localized in 8 road sections, 22 out of 444 in e-scooter tests, the most severe localized in 6 sections, and no outliers were identified in the car tests.

3.4. Speed correction

Many researchers have taken into account traveling speed affects to the extent of vibrations caused by road conditions (e.g. [26, 47]). Ahlin and Granlund [48] derived a general relationship, for the golden-car quarter model, between road roughness IRI [mm/m], speeds V (km/h), and RMS [m/s^2] in a simulation study:

$$\frac{\text{RMS}}{\text{IRI}} = 0.16 \left(\frac{V}{80} \right)^{\frac{w-1}{2}} \quad (2)$$

Eq. 2 can be used to adjust IRI reference values to provide the same RMS at a speed (V) different from the standard 80 km/h:

$$\frac{\text{IRI}_V}{\text{IRI}} = \left(\frac{V}{80} \right)^{\frac{w-1}{2}} \quad (2\text{bis})$$

Moreover, for a given IRI pavement profile, Eq. (2) shows how the RMS varies with speed following the relationship (3):

$$\frac{\text{RMS}_1}{\text{RMS}_2} = \left(\frac{V_1}{V_2} \right)^{\frac{w-1}{2}} \quad (3)$$

In Eqs. 2 and 3, w is the exponent of the road profile displacement PSD (Gd(n)) model of ISO 8608 [42]:

$$G_d(n) = G_d(n_0) \left(\frac{n}{n_0} \right)^{-w} \quad (4)$$

where.

n is the wave number [cycles/m] and.

n_0 is the reference spatial frequency ($n_0 = 0.1$ cycle/m).

The PSD slope w is low for roads where the dominating roughness amplitudes have short wavelengths (e.g. surface cracking and potholes) and higher when the dominating roughness amplitudes have long wavelengths (e.g. unevenness). A common value of w is around 2 and the value of 2 is also used in ISO 8608 for road classification (Fig. 5). However, it can be expected that the actual road PSD is not always a straight line and could be represented by a Gd(n) with variable w values in different ranges of octave bands. For example, for the test road PSD (Fig. 2) the best fitting can be obtained applying a two split straight line with two different values of w= 3.4 in the range 0.0015–0.075c/m ($R^2 = 97\%$) and w= 2.2 in the range 0.098–2.5c/m ($R^2 = 99\%$), confirming the higher complexity of road pavement surfaces in urban roads where coexistence of different distress typologies and severities are more

frequent than in principal rural roads [49]. The relationship between the speed and RMS is complex and it does not follow any pre-definite proportionality general relationship. Moreover, we have already commented as the IRI golden quarter car model is not directly applicable to bike and e-scooter. Therefore, in order to account for the effect of speed on RMS for the bike and e-scooter, we used an empirical approach, applied in other studies with cars [26,47], to estimate the exponent k in Eq. 5 in order to adjust the experimental RMS to a unique reference speed:

$$RMS_{n,i} = RMS_i \times \left(\frac{v_T}{v_i} \right)^k \quad (5)$$

where $RMS_{n,i}$ is the adjusted RMS at the target speed v_T [m/s], RMS_i is the original acceleration data at the speed v_i and k is determined iteratively to minimize the Mean Square Error (MSE). MSE is computed with Eq. 6, comparing the value recorded at the reference speed (RMS_{V_T}) with the other ones collected in the same road section at the effective speed v_i and corrected with Eq. 5 ($RMS_{n,i}$):

$$MSE = \frac{\sum_{i=1}^N (RMS_{n,i} - RMS_{V_T})^2}{N} \quad (6)$$

in which N is the total number of RMS data collected in all the test runs at various riding speed.

The reference speeds considered are 5 m/s for bike and 4 m/s for e-scooter. For comparison we carried out one test with car at a constant speed of 12 m/s that is used as reference speed for car in urban area, as well.

Curves in Fig. 7 show the existence of a minimum in the k/MSE curves which support the assumption for speed correction. The minimum was detected at the value of k equal to 1.2 for e-scooter and 1.15 for the bike. Such behavior (i.e. $k > 1.0$) in vibration amplitude related to speed is consistent with similar studies for passenger cars (i.e. $k < 1$) because of the more rigid and elastic linear response of such vehicles without an effective suspension system. To check the effectiveness of the speed correction for a homogeneous comparison of acceleration data collected by bikes and e-scooters at different speed in real world conditions, we applied the ANOVA with repeated measures, to compare RMS means of the different tests before and after correction for speed. What we expect and test, is that the statistical difference among repeated measures in the same road section at different speeds will be reduced after correction. The F test on the Sum of Squares Type III error divided by the degree of freedom, is used to show significance of the null hypothesis of equal means. Because the hypothesis of sphericity, that is not very powerful for small sample sizes, could be not satisfied [50,51], an adjustment to the degrees of freedom has been made and the significance of the F ratio was evaluated with the new degrees of freedom. The Greenhouse-Geisser adjustment is usually the less conservative, while Lower-bound is the most conservative approach. Results are reported in Table 2.

The repeated measures ANOVA determined that the statistical difference of mean RMSs is always reduced after speed correction, as showed by an increase in the p-value of the F test (we can refer to the lower-bound correction to be conservative). Before speed correction the rejection of the null hypothesis of equal mean is always more than 99.9% (p-value <0.001). The improvement in homogeneity of RMS in the different runs is strong for the bike, because we can state that, in the after condition, we can reject the null hypothesis of equal means only with 40% level of confidence (p-value 0.602). Also, the data collected with e-scooter showed a non-significant difference in the means after correction (p-value 0.088) even if with lower level of confidence than bike, but always higher than in the before condition.

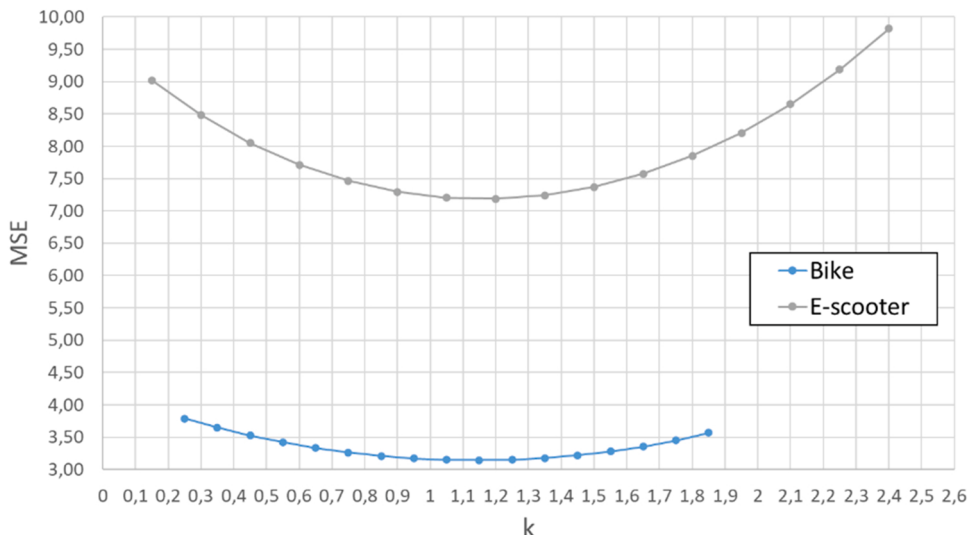


Fig. 7. Relationship between mean square error of normalized acceleration speed and power k for bike and e-scooter.

Table 2
ANOVA with repeated measures.

ANOVA BIKE		Type III Sum of Squares	df	Mean Square	F	Sig.
RMS before speed adjustment			4			
Greenhouse-Geisser	224.194	3.298		67.985	17.564	.000
Lower-bound	224.194	1.000		224.194	17.564	.000
RMS After speed adjustment			4			
Greenhouse-Geisser	3.203	3.622		.884	.274	.878
Lower-bound	3.203	1.000		3.203	.274	.602
ANOVA E-SCOOTER		Type III Sum of Squares	df	Mean Square	F	Sig.
RMS before speed adjustment			3			
Greenhouse-Geisser	258.490	1.996		129.491	14.467	.000
Lower-bound	258.490	1.000		258.490	14.467	.000
RMS After speed adjustment			3			
Greenhouse-Geisser	36.696	2.822		13.002	2.958	.036
Lower-bound	36.696	1.000		36.696	2.958	.088

3.5. Comfort level estimation

Vertical accelerations were further analyzed in terms of whole-body vibrations (WBV) for the user's comfort in transport, based on ISO 2631-1 [46]. For riders of bicycle and e-scooter, the WBV exposure produced by the pavement distress may cause not only uncomfortable feeling, but also standing balance and in the medium term cognitive/motor impairment. According to ISO standard, the way in which vibrations affect the user's comfort depends on the frequency content of the vibrations. The procedure requires the application of frequency weighting filters to the acceleration signal. Accordingly, the signal was divided into the 24 third octave bands of ISO 2631-1 available in our sampling rate [range 0.1–20 Hz]. The overall weighted RMS_w acceleration was calculated by Eq. 7:

$$RMS_w = \sqrt{\sum_i (W_i a_i)^2} \quad (7)$$

where W_i is the i^{th} frequency weighting associated with the i^{th} one-third octave band, and a_i is the RMS of vertical acceleration filtered in the same i^{th} one-third octave band. The W_i weights are valid only for people standing or in seated position, such as the regular road user.

Fig. 8 shows the distribution of the mean a_i and W_i in the 24 octave bands for the three vehicles tested in the experiment.

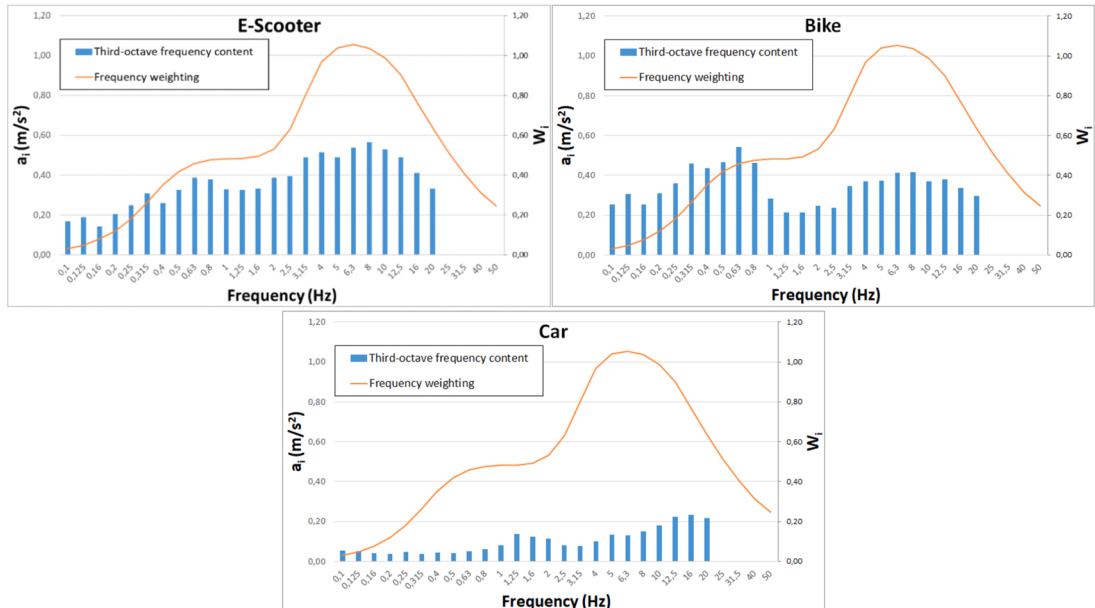


Fig. 8. Third-octave frequency a_i compared to Frequency factors in ISO 2631.

The frequencies with higher weights, effecting more the comfort, are in the range of 0.5 – 20 Hz. This is within the acquisition capabilities of smartphones and corresponds to roughness wavelengths between 0.2 and 10.0 m at a speed around 20 km/h. It is worthy to mention that mainly e-scooter showed the highest values of a_i in correspondence with the frequencies that generate more discomfort to the user.

4. Data analysis and discussion

4.1. Correlation with IRI

The correlation between vertical acceleration and pavement roughness was developed for each type of vehicle in the experiment. The correlation analysis was carried out considering for each 10 m section the IRI and the acceleration in terms of RMS corrected at the target speed. As in the data processing, outliers identified by studentized residual in the correlation estimation were identified and excluded from the analysis.

Fig. 9 shows the linear correlation coefficient estimates and R^2 for the three vehicles used. Although for the car it would have been possible to obtain a higher correlation with a different model form (e.g. 53% with a double squared model), for comparison we report only the results of the linear regression models for all the three vehicles investigated.

According to the results reported in **Fig. 9**, both bike and e-scooter showed a very weak correlation with IRI. As expected, correlation coefficient R^2 (adjusted to the degree of freedom) is higher for car ($R^2 = 0.45$) even if lower than in other studies [24,26,52]. Anyway, we can consider consistent the result because of the very short section length of 10 m, which exposes data to more variability and damping tail effects in the quarter car model.

4.2. Correlation with distress

The goal is to compare the distress extension and severity with the average value of RMS in each road sample section and to analyze the degree of correlation.

Preliminary, we checked if it is possible to merge data from bike and e-scooter to have a wider sample and to be consistent with the practical application of the procedure. The paired t-test is the statistical tool to compare sample means. Because of the presence of sections with localized distresses which can occasionally produce peak values in RMS (i.e outliers), we adopted a stratified bootstrap approach to estimate the confidence intervals of our statistics (e.g mean and correlation coefficient). Bootstrapping is a no-parametric method for deriving robust estimates of standard errors and confidence intervals as alternative to parametric estimates when the assumptions of bivariate normal distribution could be violated as in our case with heteroscedastic residuals fit to a small sample. Stratified bootstrap sampling is also useful when units within each stratum are relatively homogeneous while units across strata are different. We applied two strata by using as control factor the existence of an outlier in RMS and then the stratum-level estimates have been combined to estimate the overall correlation.

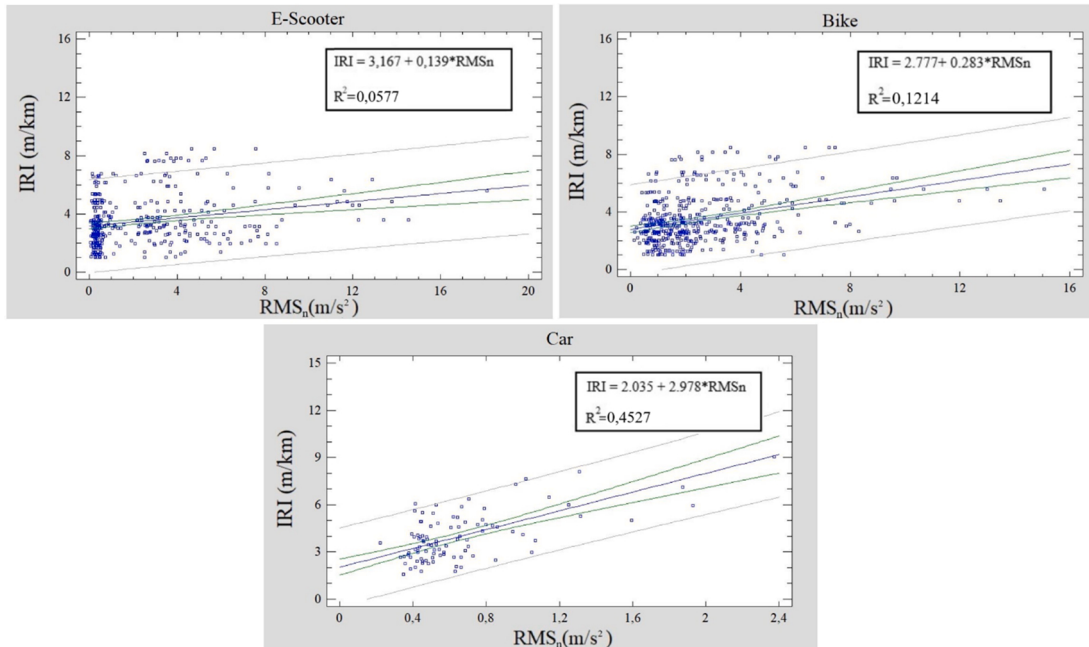


Fig. 9. Correlation between normalized RMS and IRI for bike, e-scooter and car.

The paired t-test showed that we can reject the null hypothesis of difference in the means between Bike and e-scooter RMS ([Table 3](#)), therefore the correlation analysis was carried out using the mean RMS among all the test rides. This approach is consistent with the practical perspective to collect data from a larger sample of users without the need to identify the type of two-wheel vehicle.

The Pearson's correlation coefficient and significance P-value are two measure to test the existence of linear association between RMS and distress extension. Because, the presence of localized man made (MM) pavement irregularities (e.g. gutters, service covers) has been considered as a dichotomous variable (i.e. 0: no present; 1: present), the correlation between mean RMS and MM was tested via the no-parametric Spearman rank-order correlation coefficient and significance test ([Table 4](#)). It is also worth noting that a Spearman's correlation is not very sensitive to outliers.

[Table 4](#) shows the significant and good correlation of RMS with moderate severity cracks (Longitudinal, Transversal and Alligator) and not significant or weak correlation with low severity ones. High severity longitudinal and transversal cracks (i.e. cracks with width>19 mm) and MM showed significant, but medium correlation coefficients. Potholes appear not correlated with RMS and for high severity longitudinal and transversal cracking the lower bootstrap confidence interval is close to zero (i.e. low significance over 95%).

Results of the correlation analysis confirmed the existence of correlation between distress severity and RMS useful for pavement monitoring and maintenance programs, but also the issue for a specific consideration of the RMS peaks (outliers) as KPI for the higher severity and localized distresses that are more random due to the rider tendency to avoid localized high severity distress because they are perceived as more uncomfortable and hazardous.

Pavement singularities are usually avoided by the users, but when encountered in the ride path, they will create outliers in data that can be identified to discriminate between diffused (e.g. medium severity cracking, unevenness) and localized pavement distress (e.g. high severity cracks, potholes, bumps, MM).

Existence of pavement singularities capable to produce RMS outliers can be identified comparing section where RMS outliers were identified with presence of distress in terms of type and severity. Accordingly, each pavement section was classified as Negative or Positive when with or without pavement distress of defined typology and severity. Analogously, the road section was classified as Negative or Positive when with at least one RMS outlier or always without outliers. More specifically, we compared to classification criteria. A) Negative a sample section with $RMS > 8 \text{ m/s}^2$ (corresponding to $SR>2$ in our sample) and B) $RMS > 10 \text{ m/s}^2$ (i.e. $SR>3$).

We applied the Receiving Operating Characteristics (ROC) curve method to select the best classification models and to discard suboptimal ones. The ROC curve is created by plotting the true positive rate (TPR) against the false positive rate (FPR) at various threshold settings. The true-positive rate is also known as sensitivity, recall or probability of detection:

$$TPR = TP/P = TP/TP + FN \quad (8)$$

where, for the confusion matrix, TP are True Positive, and FN are False Negative (type II error – mistaken acceptance of the null hypothesis).

The false-positive rate is also known as probability of false detection and can be calculated as $(1 - \text{specificity})$:

$$FPR = FN/P = FP/FP + TN(1 - \text{Specificity}) \quad (9)$$

where, for the confusion matrix, FP are False Positive (type I error - mistaken rejection of the null hypothesis), and TN are True Negative.

The parameter AUC (Area Under the Curve) of the ROC curve tells how much the model can distinguish between classes. Higher the AUC, the better the model is, 0.5 means a correspondence only by chance.

We compared AUCs to define which RMS thresholds and distress combination returned the best classification of outlier sections. [Table 5](#) shows the results for the best classification models.

$RMS > 8 \text{ m/s}^2$ resulted the best predictor of sections where RMS outliers are good predictors (AUC=0.756) of sections with the presence of Potholes (P) and MM, Alligator Cracking moderate (AC_M), Transversal and Longitudinal cracking with high severity (L_H, T_H) (case 1 A). These sections must be prioritized in the maintenance programs (also with short time repair treatments) because very uncomfortable and hazardous for the two-wheel users.

Table 3
Stratified Bootstrap Paired T-test of RMS means between Bike and E-scooter.

		Statistic	95% Lower Confidence Interval	95% Upper Confidence Interval	Paired T-test Sig. (2-tailed)	Bootstrap Paired T-test Sig. (2-tailed)
Sm	Mean	2.683	2.299	3.062	0.431	0.387
	Std.	2.670	2.110	3.144		
	Deviation					
Bm	Mean	2.833	2.547	3.113		
	Std.	1.981	1.587	2.354		
	Deviation					
N		111				

Table 4

Correlation of the average RMS with distress type and severity.

	Long L ⁽¹⁾	Long M ⁽¹⁾	Long H ⁽¹⁾	Trans L ⁽¹⁾	Trans M ⁽¹⁾	Trans H ⁽¹⁾	Alligator L ⁽¹⁾	Alligator M ⁽¹⁾	Potholes M ⁽²⁾	MM ⁽³⁾
Correlation coefficient	-0.01	.55	.39	.22	.51	.31	.03	.48	.07	.38
Sig. (2-tailed)	.899	< 0.001	< 0.001	.020	< 0.001	< 0.001	.732	< 0.001	.479	< 0.001
N	111	111	111	111	111	111	111	111	111	111
Bootstrap	Bias	.005	-0.017	-0.013	.006	-0.004	.022	.001	.012	-0.006
	Std. Error	.074	.119	.167	.086	.104	.135	.085	.090	.071
95% C. I.	Lower	-0.137	.257	.057	.057	.298	.071	-0.126	.280	-0.028
	Upper	.150	.732	.672	.399	.696	.591	.214	.633	.252
										.494

⁽¹⁾ Pearson Correlations; ⁽²⁾ Potholes low and high are not tested because of the limited sample size; ⁽³⁾ Spearman's statistics

Table 5

AUC for different RMS thresholds and combination of distress.

case	Distress	A. RMS > 8 m/s ²			A. RMS > 10 m/s ²		
		AUC	Sensitivity	1 - Specificity	AUC	Sensitivity	1 - Specificity
1	P + MM+AC_M+L_H+T_H	0.756	.667	.155	.752	.706	.202
2	P + MM+AC_M	0.743	.630	.143	.728	.647	.191
3	P + MM+L_H	0.661	.370	.048	.703	.471	.064
4	P + MM+T_H	0.587	.222	.048	.586	.235	.064

4.3. Rating of comfort

The results of the WBV expressed in terms of frequency-weighted RMS for each 10-meters section, have been classified with respect to the classes defined by ISO 2631-1. The comfort assessment was carried out also by using IRI with the PSR scale reported in ASTM E1927-98 [53]. Classification and threshold values are shown in (Table 6).

The overlapping zone between two adjacent classes is due to various factors, as the reactions to the RMS amplitudes depend on the expectations of the users and on variables such as the level of acoustic noise, temperature and age that could cause the perceived comfort level to vary (ISO 2631-1).

Fig. 10 shows the maps of WBV comfort levels for users on bikes, e-scooters, cars and the PSR classification based on IRI.

The increase in the number of sections considered "Extremely uncomfortable" from 0% of the car to 31% of the e-scooter and the general increase of the sections belonging to the higher classes confirms that the same conditions of the road pavement are perceived differently on-board vehicles of different characteristics (Table 7). Pavement distress that may be negligible for the comfort of the motorized vehicles (e.g. high frequency profile wave numbers, low/moderate cracks), can cause discomfort to users of bikes and e-scooter. High severity distresses make the road pavement uncomfortable for e-scooter and bike while not perceived the low speed.

Classification based on IRI/PSR scale is not consistent with comfort levels for all the vehicles including car. Comparison of actual comfort levels for car at 45 km/h test speed, with thresholds derived from IRI, must be considered with caution, because IRI is determined at a reference speed of 80 km/h. As reported in Eq. 2 at lower speed higher values of IRI can be accepted [48].

To compare correlation between the comfort ranks obtained from the different vehicles measured on a common monotonic Likert scale (0–5), the Spearman rank test was performed (Table 8).

Results of rank comparison of WBV comfort classification according to the ISO standard, showed the existence of significant correlations between the different vehicles, but the higher correlation was between bike and e-scooter scores (0.666). Instead, the correlation coefficient was low when the comparison was made between car and bike (0.316) or e-scooter (0.275). The PSR rating derived from IRI was always not significant with the ranking provided by RMS.

5. Conclusions and lessons learned

Results confirmed the lack of correlation of vibrations in bikes and e-scooter with IRI the most known standard KPI for road pavement surface, how is theoretically expected and experimentally tested in the study. Therefore, there is the need to use different KPIs for pavement management in urban areas where light-mobility needs to be more attractive for commuter and leisure users to improve transport mobility and quality of life in our cities. In such framework, the research target was to analyze the capabilities to use low cost sensors (e.g. smartphone) and light 2 wheels vehicles (i.e. bike and e-scooter) to monitor road pavement characteristics and to assess the comfortable and safety ride conditions. Despite the topic of smartphone and probe vehicles is widely discussed in the literature, in the author knowledge that is one of the few studies that combine bike and e-scooter vehicles with a detailed report of pavement conditions in terms of distress features and road profile characteristics.

RMS of vertical acceleration and ranking of comfort with weighted RMSw, according to ISO 2631-1, have been confirmed suitable KPIs of pavement conditions that can be collected by smartphone in bikes and e-scooters, providing consistent results with actual pavement distress characteristics and severity ranking. Data from bikes and e-scooter can be merged because they have given comparable and well correlated results, even if e-scooter returns higher vibration frequencies and lower comfort rating.

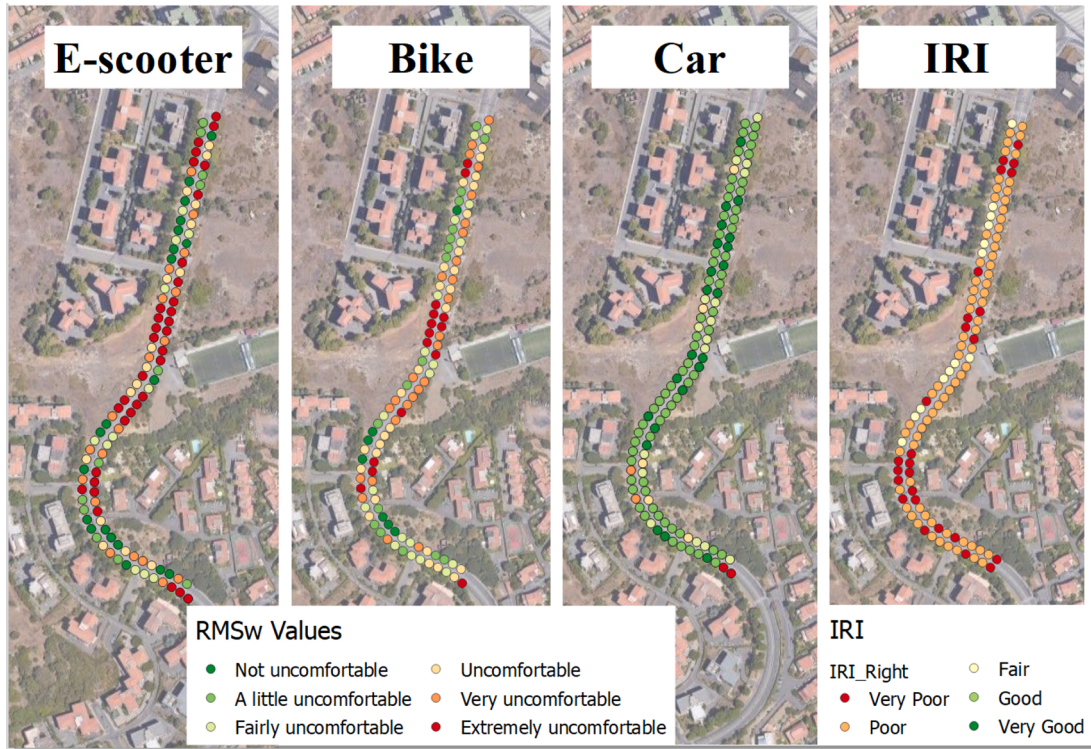
To have homogeneous results, adjustment of RMS for speed variability must be applied. A reference speed of 4 and 5 m/s was used for bike and e-scooter, respectively and an approximately linear correction factor was identified with significant improvement in homogeneity of results during repeated measures. At the usual urban speeds, they are more sensible to the high pavement wave numbers (e.g. 1.0–5.0c/m) mainly related to cracks also of moderate severity rather than medium range wave numbers (e.g. 0.03–1.0c/m) related to pavement unevenness (e.g. swelling, depressions) mainly affecting IRI and vibrations in damped vehicles. Good correlations have been identified between average RMS and medium severity cracks. Pavement singularities are usually avoided by the users, but when encountered in the ride path, they will create outliers in data that can be identified to discriminate between diffused moderate severity cracking and localized high severity pavement distress. Best predictor of high severity pavement distress was identified RMS higher than 8 m/s², which are of concern for vehicle stability and safety and caused by occasional riding over localized higher severity distress, potholes or MM. Pavement monitoring by bikes and e-scooter can provide effective detection of typologies and severities of distresses not detectable by similar approaches in damped vehicles.

In the perspective of the urban pavement management system, results showed that with appropriate data treatment and interpretation it is possible to collect useful information not only for pavement management of dedicated bike paths or lanes, but also data

Table 6

Comfort classes proposed by ISO 2631 and PSR classes from ASTM 1927–98.

RMS_w (m/s^2)	Comfort class	IRI	PSR (class)
Less than 0.315	Not uncomfortable	Less than 0.4	5 (Perfect)
0.315–0.63	Little uncomfortable	0.4–0.8	4 (Very Good)
0.5–1.0	Fairly uncomfortable	0.8–2.0	3 (Good)
0.8–1.6	Uncomfortable	2.0–4.7	2 (Fair)
1.25–2.5	Very uncomfortable	4.7–12.6	1 (Poor)
More than 2.5	Extremely uncomfortable	More than 12.6	0 (very Poor)

**Fig. 10.** Vibration comfort and PSR of sections based on ISO 2631–1.**Table 7**

Comparison of the percentage distributions of comfort rating given by the different KPIs.

	< 0,315	0,315 – 0,565	0,565 – 0,9	0,9 – 1,425	1,425 – 2,5	> 2,5
	Not uncomfortable	A little uncomfortable	Fairly uncomfortable	Uncomfortable	Very uncomfortable	Extremely uncomfortable
E-scooter	18%	10%	10%	14%	17%	31%
Bike	6%	15%	17%	24%	23%	14%
Car	20%	59%	15%	5%	2%	0%
	Perfect	Very Good	Good	Fair	Poor	Very Poor
PSR	0%	0%	12%	65%	22%	2%

about pavement surface distresses complementary to those available from standard IRI or collected with similar acquisition systems installed in passenger cars. Therefore, in urban road, pavement monitoring for preventive maintenance (e.g. resurfacing, cracking sealing, patching) is a priority not only for micro-mobility comfort and safety, but also for pavement preservation and cost optimization.

Compared to the large experience already available for cars and other motorized vehicle (e.g. Bus, Truck), spectral distribution of vibrations and ranking of comfort levels are significantly different for bike and e-scooter. Body vibration comfort was estimated according to the ISO procedure providing tailored rating for bikes and e-scooters confirmed not in agreement with the same estimation on

Table 8

Spearman's rank correlation between comfort ratings of e-scooter (es_Consort), Bike (b_Consort) and car (c_Consort).

Spearman rank Correlations			B_rating	C_rating	PSR
Spearman's rho	ES_rating	Correlation Coefficient	.666	.275	.091
		Sig. (2-tailed)	.000	.004	.342
		N	111	109	111
	B_rating	Correlation Coefficient		.316	.254
		Sig. (2-tailed)		.001	.007
	C_rating	Correlation Coefficient			.187
		Sig. (2-tailed)			.052

board of cars or based on standard IRI thresholds.

The study was developed in a controlled experiment, but lesson learned can be shared in the perspective of practical applications. Smartphone accelerometers usually don't meet the ISO 8041 [54] and ISO 2631 [46] requirements. Anyway, smartphones offer a unique solution for a wide acquisition of acceleration and GNSS position data from bikes and e-scooter where more advanced and power supply systems are not usually available. The frequency acquisition was set to 20 ms (i.e. 25 Hz signal) limiting the range of vibration frequencies to be analyzed, while covering the values more relevant for transport comfort. Nominally it is possible to increase the acquisition time of smartphone to 10 ms (i.e. 50 Hz signal) even if preliminary test showed gaps in data recording by using a Huawei P20lite. Resampling techniques and new generation of smartphone with faster CPU could mitigate the problem, anyway doubling the data sampling remains an issue to be considered in the perspective to a large number of users and extended time recording. When several users share their data, GNSS positioning can be used for clustering information and improving the reliability of the assessment. AGNSS (Augmented GNSS) and multi constellation satellites (e.g. GPS, Galileo, GLONASS, BeiDou) usually applied by modern smartphone are able to provide enough position accuracy (e.g. 2–3 m) with slight degradation in not optimal conditions of satellites view (e.g. urban canyon, trees) [11,13]. One second is the standard frequency acquisition of GNSS systems in smartphone that is enough for positioning of data also in short road sections (e.g. 2 s for 10 m data sampling, like in the present study).

At the present stage of the research and as reported in the literature, it is not possible to classify pavement distress at the same level of accuracy (e.g. extension and width of cracking, area and depth of potholes) available from direct measurements like has been done in the present study with ARAN. Anyway, basing on the results of the study, and further preliminary analysis we can expect an overall classification capability for pavement cracking of moderate and high severity which can be detected and classified by the values of RMS. While outliers are more difficult to be used for detailed classification of distress typology (e.g. potholes vs. humps) and its characteristics (e.g. pothole area and depth).

In this perspectives, extension of quality database with different distress typologies and severities, as proposed in the present study, can provide a suitable set of data also to apply advanced artificial intelligence classification techniques.

CRediT authorship contribution statement

Conceptualization: SC, GP, AD; Methodology: SC, GP; Investigation: GP, VM; Data curation and formal analysis: VM; Statistical analysis: GP; Writing – original draft preparation: GP, VM.; Writing-review and editing, SC, AD; Project administration and funding acquisition: SC, AD. All authors have read and agreed to the published version of the manuscript.

Declaration of Competing Interest

The authors declare that they have no known competing financial interests or personal relationships that could have appeared to influence the work reported in this paper.

Acknowledgments

This work has been partially financed by the Italian Ministry of Research project PRIN 2017 USR342 and “Astro Database” Project of the University of Catania, project TIMUC (PIACERI) by the University of Catania.

References

- [1] J. Pucher, R. Buehler, Cycling towards a more sustainable transport future, *Transp. Rev.* 37 (6) (2017) 689–694, <https://doi.org/10.1080/01441647.2017.1340234>.
- [2] A. Feizi, J.S. Oh, V. Kwigizile, S. Joo, Cycling environment analysis by bicyclists' skill levels using instrumented probe bicycle (IPB), *Int. J. Sustain. Transp.* 14 (9) (2020) 722–732, <https://doi.org/10.1080/15568318.2019.1610921>.
- [3] AASHTO, Guide for the Development of Bicycle Facilities. 2012. Available on: (<https://njdotlocalaidrc.com/perch/resources/aashto-gbf-4-2012-bicycle.pdf>) Accessed 26 July 2021.
- [4] Austroads, Guide to Road Design Part 6A: Paths for Walking and Cycling. 2021. Available on: (<https://bicycleinfrastructuremanuals.com/manuals3/Austroads%20Paths%20for%20Walking%20and%20Cycling.pdf>) Accessed 26 July 2021.
- [5] Austroads, Cycling Aspects of Austroads Guides. 2017. Available on: (<https://austroads.com.au/publications/traffic-management/ap-g88-17>) Accessed July 23, 2021.

- [6] W. Uddin, W. Hudson, R. Haas, Framework for infrastructure asset management. In public infrastructure asset management, second ed., McGraw-Hill Education,, Columbus, OH, USA, 2013.
- [7] A. Di Graziano, V. Marchetta, S. Cafiso, Structural health monitoring of asphalt pavements using smart sensor networks: a comprehensive review, *J. Traffic Transp. Eng.* 7 (5) (2020) 639–651, <https://doi.org/10.1016/j.jtte.2020.08.001>.
- [8] Austroads, Research Report AP-R651-21 Next Generation Asset Data Collection Pavement Performance. 2021. Available on: (<https://austroads.com.au/publications/asset-management/ap-r651-21>). Accessed 18 July 2021.
- [9] S.R. Singiresu , Mechanical vibrations. Boston, 1995.
- [10] S.V. Kumar, Bicycle ride comfort evaluation and optimization, *Univ. Prestori, Res. Rep.* (2019), <https://doi.org/10.13140/RG.2.2.26063.64162>.
- [11] N. Stamatiadis , G. Pappalardo and S. Cafiso , Use of technology to improve bicycle mobility in smart cities, 5th IEEE Int. Conf. Model. Technol. Intell. Transp. Syst. MT-ITS 2017 - Proc., pp. 86–91, 2017, doi: 10.1109/MTITS.2017.8005636.
- [12] J. Gao, A. Sha, Y. Huang, L. Hu, Z. Tong, W. Jiang, Evaluating the cycling comfort on urban roads based on cyclists' perception of vibration, *J. Clean. Prod.* 192 (2018) 531–541, <https://doi.org/10.1016/j.jclepro.2018.04.275>.
- [13] N. Stamatiadis, S. Cafiso, G. Pappalardo, A comparison of bicyclist attitudes in two urban areas in USA and Italy, *Adv. Intell. Syst. Comput.* 879 (2019) 272–279, https://doi.org/10.1007/978-3-030-02305-8_33.
- [14] J.D. Cano-Moreno , M.I. Marcos , F.B. Haro , R. D'Amato , J.A. Juanes and E.S. Heras , Methodology for the study of the influence of e-scooter vibrations on human health and comfort, *ACM Int. Conf. Proceeding Ser.*, pp. 445–451, 2019, doi: 10.1145/3362789.3362906.
- [15] Q. Ma, H. Yang, A. Mayhue, Y. Sun, Z. Huang, Y. Ma, E-Scooter safety: The riding risk analysis based on mobile sensing data, *Accid. Anal. Prev.* 151 (2020) (2021), 105954, <https://doi.org/10.1016/j.aap.2020.105954>.
- [16] D. Lee, I. Kim, M. Hahn, Trajectory-based road-geometry and crash-risk estimation with smartphone-assisted sensor networks, *Int. J. Distrib. Sens. Netw.* 2014 (2014), 943845, <https://doi.org/10.1155/2014/943845>.
- [17] S. Cafiso, A. Di Graziano, R. Fedele, V. Marchetta, F. Praticò, Sensor-based pavement diagnostic using acoustic signature for moduli estimation, *Int. J. Pavement Res. Technol.* 13 (6) (2020) 573–580, <https://doi.org/10.1007/s42947-020-6007-4>.
- [18] P. Mohan , V.N. Padmanabhan , R. Ramjee , TrafficSense: Rich Monitoring of Road and Traffic Conditions using Mobile Smartphones, *Proceedings of the 6th International Conference on Embedded Networked Sensor Systems, SenSys 2008*, Raleigh, NC, USA, November 5–7, 2008, doi: 10.1145/1460412.1460444.
- [19] A. Chatterjee, Y.J. Tsai, Training and testing of smartphone-based pavement condition estimation models using 3D pavement data, *J. Comput. Civ. Eng.* 34 (6) (2020) 1–11, [https://doi.org/10.1061/\(ASCE\)CP.1943-5487.0000925](https://doi.org/10.1061/(ASCE)CP.1943-5487.0000925).
- [20] J. Eriksson, , L. Girod , B. Hull , R. Newton , S. Madden , H. Balakrishnan , The Pothole Patrol: Using a Mobile Sensor Network for Road Surface Monitoring, *Proceedings of the 6th International Conference on Mobile Systems, Applications, and Services (MobiSys 2008)*, Breckenridge, CO, USA, June 17–20, 2008, pp. 29–39, 2008, doi: 10.1145/1378600.1378605.
- [21] A. Mednis, , G. Strazzins , R. Zviedris , G. Kanonirs , L. Selavo , Real Time Pothole Detection using Android Smartphones with Accelerometers, *International Conference on Distributed Computing in Sensor Systems and Workshops (DCOSS)*, 2011, doi: 10.1109/DCOSS18718.2011.
- [22] V. Astarita, R. Vaiana, T. Iuele, M. Caruso, V. Giofrè, F. De Masi, Automated sensing system for monitoring of road surface quality by mobile devices, *Procedia - Soc. Behav. Sci.* 111 (2014) 242–251, <https://doi.org/10.1016/j.sbspro.2014.01.057>.
- [23] L. Janani, V. Sunitha, SamsonMathew, Effect of combining algorithms in smartphone based pothole detection, *Int. J. Pavement Res. Technol.* 14 (2021) 63–72, <https://doi.org/10.1007/s42947-020-0033-0>.
- [24] S.F. Yeganeh, A. Mahmoudzadeh, A. Golroo, Validation of smartphone-based pavement roughness measures, *AJCE* 1 (2) (2019) 135–144, <https://doi.org/10.22060/ajce.2017.13105.5328>.
- [25] G. Alessandroni, et al., Smartroadsense: collaborative road surface condition monitoring, *Second IEEE SPS Italy Chapter Summer Sch. Signal Process.* (2014) 210–215, <https://doi.org/10.13140/RG.2.2.29144.90881>.
- [26] H. Zeng, H. Park, M.D. Fontaine, B.L. Smith, K.K. McGhee, Identifying deficient pavement sections using an improved acceleration-based metric, *Transp. Res. Rec.: J. Transp. Res. Board* 2523 (1) (2015) 133–142, <https://doi.org/10.3141/2523-15>.
- [27] L. Forslöf, Growth medium sterilization using decomposition of peracetic acid for more cost-efficient production of omega-3 fatty acids by Aurantiochytrium, *Roadroid Contin. Road. Cond. Monit. Smart Phones* 41 (2013) 1–9, <https://doi.org/10.17265/1934-7359/2015.04.012>.
- [28] F. Seraj, N. Meratnia , P.J.M. Havinga , RoVi: Continuous Transport Infrastructure Monitoring Framework For Preventive Maintenance, 2017 IEEE Int. Conf. Pervasive Comput. Commun., pp. 217–226, 2017, doi: 10.1109/PERCOM.2017.7917868.
- [29] J.Y.M. Nuñez, D.R. Bisconsini, A.N. Rodrigues da Silva, Combining environmental quality assessment of bicycle infrastructures with vertical acceleration measurements, *Transp. Res. Part A Policy Pract.* 137 (2020) 447–458, <https://doi.org/10.1016/j.tra.2018.10.032>.
- [30] K. Zang, J. Shen, H. Huang, M. Wan, J. Shi, Assessing and mapping of road surface roughness based on GPS and accelerometer sensors on bicycle-mounted smartphones, *Sensors* 18 (3) (2018), <https://doi.org/10.3390/s18030914>.
- [31] H. Li, J. Harvey, Z. Chen, Y. He, T.J. Holland, S. Price, K. McClain, Measurement of pavement treatment macrotexture and its effect on bicycle ride quality, *Transp. Res. Rec.* 2525 (1) (2015) 43–53, <https://doi.org/10.3141/2525-05>.
- [32] M. Bíl, R. Andrášik, J. Kubecák, How comfortable are your cycling tracks? a new method for objective bicycle vibration measurement, *Transp. Res. Part C. Emerg. Technol.* 56 (2015) 415–425, <https://doi.org/10.1016/j.trc.2015.05.007>.
- [33] X. Li, D.W. Goldberg, Toward a mobile crowdsensing system for road surface assessment, *Comput. Environ. Urban Syst.* 69 (2017) (2018) 51–62, <https://doi.org/10.1016/j.compenvurbsys.2017.12.005>.
- [34] A. Shtayat, S. Moridpour, B. Best, Using e-bikes and private cars in dynamic road pavement monitoring, *Int. J. Transp. Sci. Technol.* (xxxx) (2021), <https://doi.org/10.1016/j.ijst.2021.03.004>.
- [35] M. Meocci, V. Branzi, A. Sangiovanni, An innovative approach for high-performance road pavement monitoring using black box, *J. Civ. Struct. Health Monit.* 11 (2021) 485–506, <https://doi.org/10.1007/s13349-020-00463-8>.
- [36] X. Li, D.W. Goldberg, Toward a mobile crowdsensing system for road surface assessment, *Comput. Environ. Urban Syst.* 69 (2018) 51–62, <https://doi.org/10.1016/j.compenvurbsys.2017.12.005>.
- [37] T. Nguyen, B. Lechner, Y.D. Wong, Response-based methods to measure road surface irregularity: a state-of-the-art review, *Eur. Transp. Res. Rev.* 11 (2019) 43, <https://doi.org/10.1186/s12544-019-0380-6>.
- [38] M.A. Agebure , E.O. Oyetunji , E.Y. Baagyeire , A three-tier road condition classification system using a spiking neural network model, *Journal of King Saud University – Computer and Information Sciences*, in press.
- [39] A. Basavaraju, J. Du, F. Zhou, J. Ji, A machine learning approach to road surface anomaly assessment using smartphone sensors, *IEEE Sens. J.* 20 (5) (2020) 2635–2647, <https://doi.org/10.1109/JSEN.2019.2952857>.
- [40] S. Cafiso, A. Di Graziano, D.G. Goulias, C. D'Agostino, Distress and profile data analysis for condition assessment in pavement management systems, *Int. J. Pavement Res. Technol.* 12 (5) (2019) 527–536, <https://doi.org/10.1007/s42947-019-0063-7>.
- [41] J.S. Miller, W.Y. Bellinger, *Distress identification manual for the long-term pavement performance program*, Rep. No. FHWA-HRT (2003) 13–092.
- [42] International Organization for Standardization, ISO 8608 - Mechanical vibration — Road surface profiles — Reporting of measured data, vol. E, p. 44, 2016, [Online]. Available: (<https://us.v-cdn.net/6030008/uploads/editor/83/oyhfu0i29vek.pdf>).
- [43] M.W. Sayers, S.M. Karamihas, *The little book of profiling, Basic Inf. Meas. Interpret. Road. Profiles* (1998) 100.
- [44] ASTM E1926–08, Standard Practice for Computing International Roughness Index of Roads from Longitudinal Profile Measurements 1, *ASTM Int.*, vol. i, no. Reapproved 2021, pp. 1–16, 2021, doi: 10.1520/E1926-08R21.
- [45] E. Murgano, R. Caponetto, A. Severino, G. Pappalardo, S.D. Cafiso, A novel acceleration signal processing procedure for cycling safety assessment, *Sensors* 21 (12) (2021) 1–20, <https://doi.org/10.3390/s21124183>.
- [46] International Organization for Standardization, ISO2631-1: Mechanical Vibration and Shock—Evaluation of Human Exposure to Whole-Body Vibration—Part 1: General Requirements. 2014.

- [47] C.-P. Chou, G.-J. Siao, A.-C. Chen, C.-C. Lee, Algorithm for estimating international roughness index by response-based measuring device, *J. Transp. Eng. Part B Pavements* 146 (3) (2020), 04020031, <https://doi.org/10.1061/jpeodx.0000183>.
- [48] K. Ahlin, N.O.J. Granlund, Relating road roughness and vehicle speeds to human whole body vibration and exposure limits, *Int. J. Pavement Eng.* 3 (4) (2002) 207–216, <https://doi.org/10.1080/10298430210001701>.
- [49] P. Andrén, Power spectral density approximations of longitudinal road profiles, *Int. J. Veh. Des.* 40 (1–3) (2006) 2–14, <https://doi.org/10.1504/IJVD.2006.008450>.
- [50] J.W. Mauchly, Significance test for sphericity of a normal n-variate distribution, *Ann. Math. Stat.* 11 (2) (1940) 204–209.
- [51] H. Huynh, G.K. Mandeville, Validity conditions in repeated measures designs, *Psychol. Bull.* 86 (5) (1979) 964–973, <https://doi.org/10.1037/0033-2909.86.5.964>.
- [52] G. Loprencipe, F.G.V. de Almeida Filho, R.H. de Oliveira, S. Bruno, Validation of a low-cost pavement monitoring inertial-based system for urban road networks, *Sensors* 21 (9) (2021) 3127, <https://doi.org/10.3390/s21093127>.
- [53] ASTM 1927–98, Standard guide for conducting subjective pavement ride quality ratings, ASTM Int., 2008.
- [54] International Organization for Standardization, ISO 8041 - Human response to vibration — Measuring instrumentation —, 2017, 2017.